Energy, Mines and Resources Canada | Énergie, Mines et Ressources Canada

CANMET

Canada Centre for Mineral and Energy Technology | Centre canadien de la technologie des minéraux et de l'énergie

AN EVALUATION OF THE NOTCH TOUGHNESS OF THE HEAT AFFECTED ZONE IN HY AND HSLA STEELS

J.T. BOWKER, M.W. LETTS, J.A. GIANETTO and R.F. ORR
WELDING SECTION

SEPTEMBER 1987

19 pp

PHYSICAL METALLURGY RESEARCH LABORATORIES

REPORT: PMRL 87-54(TR)

89-00981/

PHYSICAL METALLURGY RESEARCH LABORATORIES
REPORT: PMRL 87-54 (TR)

AN EVALUATION OF THE NOTCH TOUGHNESS OF THE HEAT AFFECTED ZONE IN HY AND HSLA STEELS

by

J.T. BOWKER, M.W. LETTS, J.A. GIANETTO and R.F. ORR

ABSTRACT

Using the Gleeble 1500 thermal/mechanical simulator the coarse-grain heat-affected zone region (CGHAZ) was simulated in the more conventional HY80, HY100 and Q1N high strength steels for naval application. The notch toughness properties of the CGHAZ of these steels were compared with that of the lower carbon precipitation hardened HSLA80 steel.

The CGHAZ of the HSLA80 steel had a significantly higher toughness than the HY and Q1N steels in specimens simulated at an energy input of 2 kJ/mm. At an energy input of 4 kJ/mm all of the steels had poor toughness in the CGHAZ. The toughness results are explained on the basis of microstructural characteristics.

LABORATOIRES DE RECHERCHE EN MÉTALLURGIE PHYSIQUE

RAPPORT: PMRL 87-54(TR)

ÉVALUATION DE LA RESISTANCE À L'ENTAILLE DE LA ZONE THERMIQUEMENT AFFECTÉE DAND DES ACIERS HY ET HSLA

par

J.T. BOWKER, M.W. LETTS, J.A. GIANETTO et R.F. ORR

RÉSUMÉ

À l'aide du simulateur thermique-mécanique Gleeble 1500, on a simmulé la zone thermiquement affectée à grain grossier (ZATAGG) dans des aciers de haute résistance plus conventionnels, HY80, HY100 et Q1N utilisés à des fins navales. La résistance à l'entaille de la ZTAGG de ces aciers a été comparée à celle de l'acier HSLA80 à teneur plus faible en carbone et durci par précipitation.

La tenacité de la ZTAGG de l'acier HSLA80 était considérablement plus élevée que les aciers HY et Q1N dans des échantillons simulés à un apport énergétique de 2 kJ/mm. À un apport énergétique de 4 kJ/mm, tous les aciers présentaient une faible tenacité dans la ZTAGG. Les résultats de tenacité sont expliqués en fonction des caractéristiques de la microstructure.

INTRODUCTION

This paper deals with recent advances made towards understanding the microstructure/property relationships of weld heat-affected zones (HAZ) in high-strength HY80, HY100 and HSLA80 steels. Simulated coarse-grained heat-affected zone (CGHAZ) structures were produced as a function of weld energy input in order to compare the microstructures and resultant notch toughness properties of steels being considered for naval applications. The targeted notch toughness properties for the HAZ were obtained from consideration of current military standards for submarine construction MIL-STD-1688(SH) (1) and weld metal consumable qualification MIL-E-23765/2C (2). At present military standards do not require Charpy impact testing of the HAZ region and specific requirements are unresolved. The latter specification (2) requires weld metal impact energies of 47 J at -50°C and 81 J at -18°C. Therefore, these targeted values were used for the purpose of comparison and evaluation of the HAZ toughness.

EXPERIMENTAL

Base Materials

The heat-affected-zone microstructure/property relationships were evaluated for a range of high-strength steels. The chemical composition of the steels which included HY80, Q1N, HY100 and HSLA80, are listed in Table 1. The HY80, Q1N and HY100, are conventional low-alloy high-strength quenched and tempered steels with minimum 552 and 689 MPa yield strength, respectively. These steels achieve their respective yield strength from the bainitic-martensitic duplex microstructures developed after heat treating. The Q1N steel represents the British equivalent of HY80, however with a significantly lower sulfur content. HSLA 80 is a low carbon modified version of ASTM A710 Grade A Class 3 steel. The HSLA80 steel derives its strength from copper precipitation after heat treatment.

Simulation of the CGHAZ

The Gleeble 1500 thermal/mechanical simulator was used to simulate the coarse grained heat-affected-zone (CGHAZ) in the high strength steels. The simulation parameters consisted of a peak temperature of 1350°C and cooling times $\Delta t_{800\text{-}500}$ of 11 and 45 s which correspond to the cooling rates associated with submerged-arc welding 25 mm thick plate at energy inputs of 2 and 4 kJ/mm, respectively. All Gleeble specimens were machined from the base materials with the long axis transverse to the plate rolling direction.

Following simulation the specimens were notched through-thickness for Charpy-V-notch testing. Charpy transition curves were generated for each test condition by testing three specimens per temperature at key temperatures between -80 to + 20°C.

Specimens from each test condition were prepared by standard metallographic techniques to evaluate and characterise the microstructures. Microhardness measurements were made using a 500 g load and are expressed as Vickers hardness numbers. Scanning electron microscopy (SEM) was employed to examine fracture surfaces of selected Charpy specimens.

Dilatometry

In order to better identify and characterize the microstructural constituents developed in the HAZ of the HSLA 80 steel, dilatometric experiments were performed using the Gleeble 1500 thermal/mechanical simulator. Standard Gleeble specimens (10 x 10 x 75 mm) were machined round to diameters between 6-10 mm over a length of 20 mm at the mid-span of each sample. HAZ simulation was carried out with a peak temperature of 1350°C and cooling times Δt 800-500 of 5, 11, 25, 45, 75 and 200 s to cover a wide transformation range. Duplicate tests were performed for each simulation condition and transformation temperature data was obtained from dilatometric curves.

Specimens from each test condition were sectioned transverse to the length and prepared by standard metallographic techniques. The general structure was observed after etching in 2% nital. Further details were revealed by scanning electron microscopy after etching more deeply.

RESULTS

CGHAZ Notch Toughness Properties

Charpy impact transition curves of the simulated CGHAZ for the various steel compositions are shown in Figs. 1, 2, and 3. Only the HSLA80 steel simulated at the energy input of 2 kJ/mm met the targeted HAZ notch toughness of 47 J at -50°C and 81 J at -18°C. There was no change in notch toughness properties with energy input for either the HY80 or the HY100 steels. The CGHAZ toughness for the Q1N steel also did not vary significantly with energy input, but the overall level of toughness was higher than either the HY80 or HY100 steels.

The CGHAZ of the HSLA80 steel simulated at the energy input of 2 kJ/mm had considerably higher toughness compared with that of the HY series and Q1N steels over the full test temperature range Fig. 3. For specimens subjected to the 4 kJ/mm simulation, the notch toughness decreased sharply at temperatures <10°C.

CGHAZ MICROSTRUCTURE

A predominately martensitic microstructure in the CGHAZ was observed at both the 2 and 4 kJ/mm energy input simulations for the HY80, HY100 and Q1N steels. This structure is shown typically in Fig. 4. The microhardness readings for these simulated HAZ specimens were in excess of 400 DPH as indicated in Table 2. SEM observations of fractured surfaces Fig. 5 and optical metallography revea'ed the presence of intercrystalline facets caused by liquation micro-cracking in the simulated HY80, HY100 and Q1N specimens. However Q1N contained a significantly lower proportion of intercrystalline discontinuities compared with HY80 and HY100.

The microstructure of the CGHAZ of the HSLA80 steel was composed of a mixture of bainite and some low carbon martensite regions after simulation at 2 kJ/mm. Using the terminology of Torronen (3) the martensitic structure in Fig. 6(a) consisted of elongated packets or laths which formed in bundles within prior austenite grains. Although transmission electron microscopy was not employed to measure the orientation relationship between adjacent packets it was assumed, based upon other studies of low carbon martensite (3, 4) and from SEM observations of fractured surfaces, that the boundaries between packets were mainly high angled.

The CGHAZ of the HSLA80 steel contained entirely coarse bainite after simulation at 4 kJ/mm. This bainitic structure, shown in Fig. 6(b), consisted of parallel bainitic ferrite laths separated by elongated martensite-austenite (MA) regions. The misorientations between adjacent laths are assumed to be low angle boundaries from fractographic evidence and electron diffraction results in other investigations of bainitic microstructure (5). For the bainitic microsturcture, a packet consists of a group of parallel laths. As shown in Fig. 6(b) a prior austenite grain may contain one or as many as three packets.

The SEM observations of the fractured surfaces of the HSLA80 simulated specimens provide evidence of the unit fracture length or cleavage facet size associated with low temperature fracture as well as the relative misorientation between packets for both the martensitic and bainitic microstructures. The cleavage facets for the 2 kJ/mm simulated specimens, shown in Fig. 7(a), were elongated and ranged in width from 5 to 10 μm. These features compare with the shape and dimensions of the individual martensitic packets shown in Fig. 6(a). The much larger cleavage facets (40 to 80 μm) observed in the fractured 4 kJ/mm simulated specimens, Fig. 7(b) relate to the bainitic packet size shown in Fig. 6(b).

The CCT diagram shown in Fig. 8 provides supporting evidence for the microstructural observations made on specimens simulated at 2 kJ/mm and 4 kJ/mm

i.e. $\Delta t_{800-500}$ =11 s and 45 s respectively. At 2 kJ/mm the microstructure consists of ~30% martensite and ~70% bainite whereas at 4 kJ/mm it is almost 100% bainitic. As the cooling time decreases below 11 s the microstructure becomes progressively more martensitic reaching 100% at $\Delta t_{800-500}$ of 4 s (equivalent to a heat input of ~1 kJ/mm on 25 mm plate). Fig. 9 shows the typical microstructure for $\Delta t_{800-500}$ of 5 s. Increasing heat input beyond 4 kJ/mm produces coarsening of the bainite microstructure and the formation of grain boundary ferrite. Figure 10 provides an example of this type of microstructure, the cooling time in this case being 75 s. Table 3 presents the results of microhardness measurements taken from specimens with cooling times in the range 5 s - 200 s. It can be seen that there is a decrease in average hardness with increasing cooling time from 5 to 45 s associated with a decrease in the proportion of martensite. For cooling times greater than 45 s the hardness is fairly constant at about 240 DPH.

DISCUSSION

The notch toughness properties of the CGHAZ of the various high strength steels can be explained on the basis of microstructural characteristics. For the higher carbon, hardenable quenched and tempered HY series steels, it was felt from previous work (6,7), that the liquation of sulphide inclusions in the CGHAZ during welding was a significant factor in lowering the notch toughness properties of this region. The sulphides which melt in the HAZ near the fusion line during welding penetrate and weaken austenitic grain boundaries by forming sulphide films during cooling (8,9). The tensile stresses generated in the welding cycle can produce discontinuities or microcracking along grain boundaries in the CGHAZ. Liquation embrittlement in the HAZ of HY80 weldments has been shown to increase with increasing carbon content and to decrease with increasing Mn/S ratio (10). The study of Q1N steel with a lower sulphur (0.005%) and higher Mn/S ratio (58/1) was intended to reduce liquation embrittlement in the CGHAZ and hence to significantly improve the notch toughness properties. The notch toughness results in Fig. 1 indicate an improvement in toughness in the Q1N Gleeble simulated specimens compared with the HY80 steel but the notch toughness properties of the CGHAZ were still below the targeted values despite the reduction in liquation embrittlement. For the HY100 steel, the tendency for liquation embrittlement in the CGHAZ had been reduced as a result of a higher Mn/S ratio (see Table 1). Therefore, one can conclude for the HY and Q1N steels,that the presence of high carbon untempered martensite in the CGHAZ makes the most significant contribution to the overall low notch toughness properties.

The prior austenite grain size of the CGHAZ of HSLA80 simulated at 2 and 4 kJ/mm are similar since they were heated to the same peak temperature of 1350°C. The excellent notch toughness properties of the CGHAZ of the HSLA80 steel subjected to Gleeble simulation of 2 kJ/mm particularly at low temperatures can be attributed to the characteristics of the low carbon martensite which makes up ~30% of the structure. It was determined from SEM examination of the fractured surface that there were two size ranges of cleavage facets. The first corresponded to the dimensions of the martensite packets i.e. 5 to 10 μm and the second much larger associated with packets of the bainitic microstructure. When cleavage fracture initiates within a packet it must reinitiate at each high angle packet boundary in order to continue propagation through the CGHAZ. The finer the packet size the higher the resistance to cleavage fracture thus the presence of ~30% low carbon martensite is sufficient to impact good notch toughness. The coarse, bainitic structure developed in the CGHAZ of the HSLA80 steel subjected to the 4 kJ/mm simulation was responsible for the poor low temperature notch toughness properties. The large cleavage facets observed in the fractured specimens are formed when a crack initiates in a packet and propagates with little resistance across the low angle boundaries which separate the parallel laths within a packet. Reinitiation takes place at the high angle packet boundaries.

CONCLUSIONS

1. In the energy input range of 2 to 4 kJ/mm the Gleeble simulated CGHAZ of the HY80, HY100 and Q1N high strength steels had poor notch toughness properties which were significantly below the targeted levels of 47 J at -50°C and 81 J at -18°C.

2. Although the formation of liquation cracking in the CGHAZ was reduced as the sulphur level was lowered in the HY and Q1N steels, the overall low toughness properties of the CGHAZ were attributed primarily to the formation of hard, untempered martensite.

3. The HSLA80 steel subjected to Gleeble simulation at 2 kJ/mm exhibited excellent notch toughness in the CGHAZ exceeding the targeted values. The low carbon martensite microstructure conferred effective fracture resistance.

4. Under high energy input conditions (4 kJ/mm) the HSLA80 steel had poor HAZ

toughness. The coarse upper bainite microstructure was responsible for the low toughness of the CGHAZ.

5. The CCT diagram of the simulated CGHAZ of HSLA80 showed that for low energy input (<1 kJ/mm) the microstructure is predominantly low carbon martensite. The microstructure becomes more bainitic with increasing heat input, reaching 100% coarse upper bainite at ~4 kJ/mm. Further increase in heat input results in the formation of grain boundary ferrite and a general coarsening of the bainite microstructure.

REFERENCES

1. U.S. Dept. of Defence, Military Specification MIL-STD-1688(SH), 1981.

2. U.S. Dept. of Defence, Military Specification MIL-E-23765/2C (SH) June, 1983.

3. K. Torronen; Microstructural Parameters and Yielding in Quenched and Tempered Cr-Mo-V Pressure Vessel Steel, Research Centre of Finland, 1979, Publ. 22.

4. M.J. Roberts; Met. Trans., 1970, Vol. 1, pp. 3287-3294.

5. F.B. Pickering; Transformation and Hardenability in Steels, Climax Molybdenum Co. of Michigan Symp., 1967, pp. 109-129.

6. K. Romhanyi, M.R. Krishnadev, R.D. McDonald, J.T. Bowker and J.T. McGrath; Microstructural Science, 1985, Vol. 14, pp. 115-126.

7. J.T. McGrath, J.A. Gianetto, R.F. Orr and M.W. Letts; Can. Met. Quarterly, 1986, Vol. 25, No.4, 1986, pp. 349-356.

8. R.H. Phillips and M.F. Jordan; Metals Tech., 1976, Vol. 3, pp. 571-579.

9. R.H. Phillips and M.F. Jordan; Metals Tech., 1977, Vol. 4, pp. 396-405.

10. C.F. Meitzner and R.D. Stout; Weld, J., 1966, Vol. 45, pp. 393-S-400-S.

Table 1 - Chemical composition of high-strength steels

Base Metal	Element wt %										
	C	Mn	Si	S	P	Ni	Cr	Mo	Cu	V	Nb
HY80	0.17	0.30	0.19	0.014	0.007	2.59	1.53	0.42	0.03	0.010.	0.005
Q1N	0.17	0.29	0.25	0.005	0.010	2.66	1.39	0.36	0.07	0.010.	0.015
HY100	0.17	0.33	0.23	0.008	0.010	2.62	1.52	0.48	0.04	0.005.	0.012
HSLA80	0.06	0.50	0.27	0.004	0.007	0.92	0.66	0.25	1.02	0.005.	0.044

Table 2 - Microhardness of as-received and simulated CGHAZ in the high-strength steels

Base metal	Microhardness, DPH		
	As-received	Simulated CGHAZ 2 kJ/mm	4kJ/mm
HY80	217	410	409
Q1N	241	429	419
HY100	287	452	450
HSLA80	246	288	242

Table 3 - Microhardness of the simulated CGHAZ of HSLA80

Δt 800 - 500(s)	Microhardness (DPH)
5	316
11	288
25	275
45	247
75	232
200	241

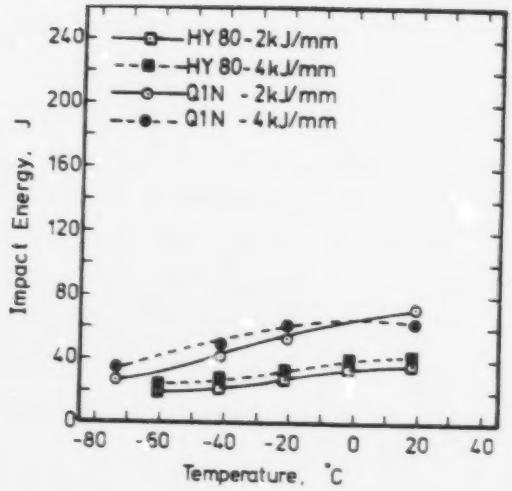

Fig. 1. Charpy transition curves of simulated CGHAZ in HY80 and Q1N steels. (neg 15284)

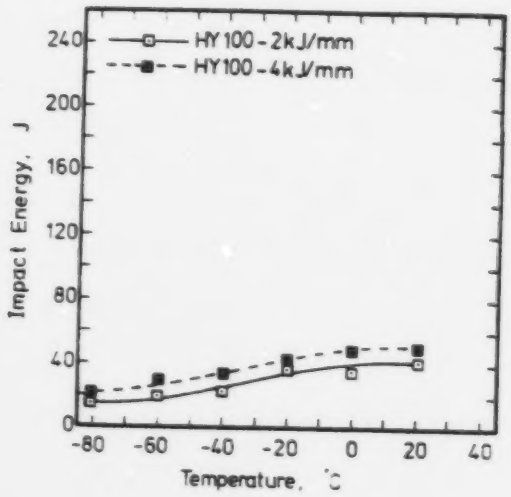

Fig. 2. Charpy transition curves of sin...lated CGHAZ in HY100 steel. (neg 15285)

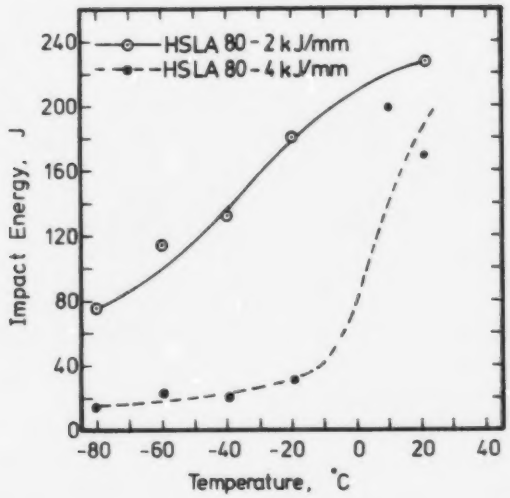

Fig. 3. Charpy transition curves of simulated CGHAZ in HSLA80 steel. (neg 15286)

Fig. 4. Microstructure of simulated CGHAZ in HY80 cycled at 4 kJ/mm. (neg 14661)

Fig.5. SEM fractograph showing intercrystalline facets on fracture surface of HY80 steel.

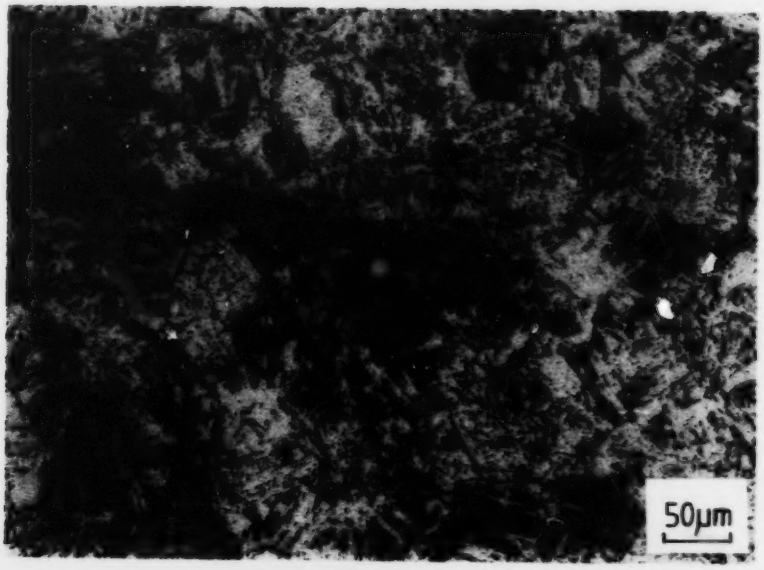

(a) 2 kJ/mm (neg 15376)

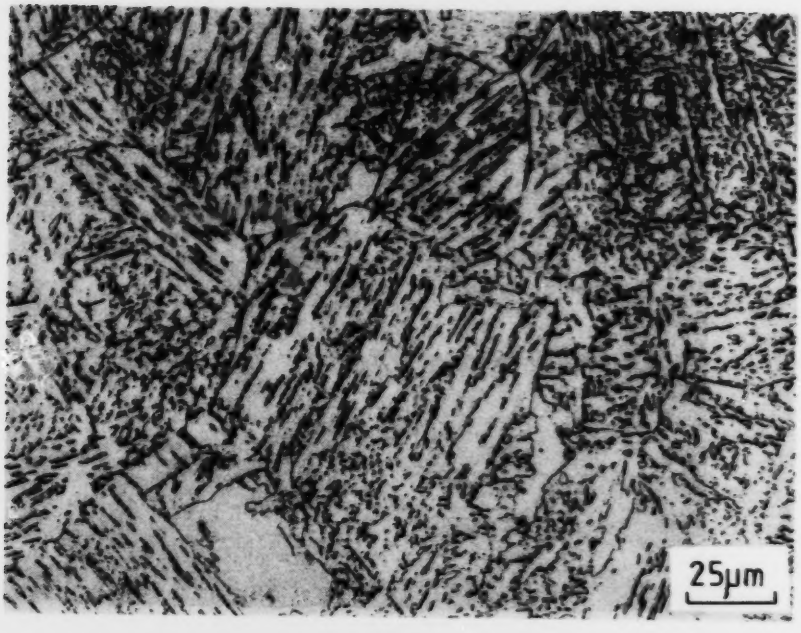

(b) 4 kJ/mm (neg 15375)

Fig. 6. Opitcal micrographs of simulated CGHAZ of HSLA80.

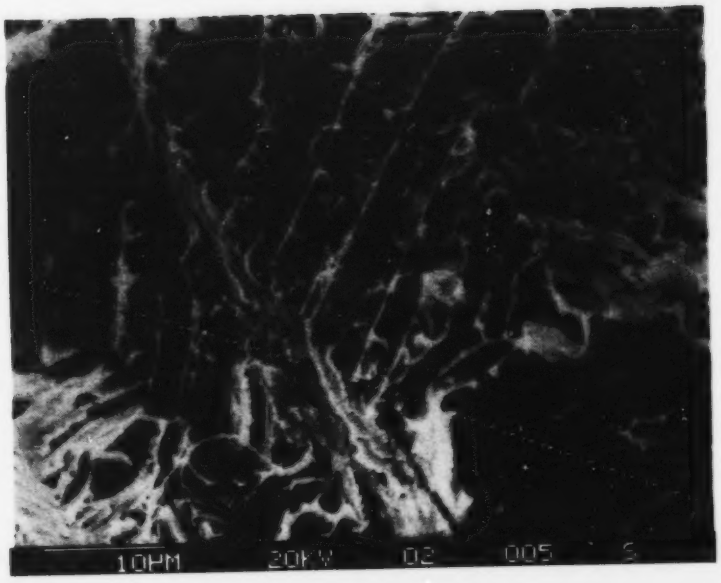

(a) 2 kJ/mm

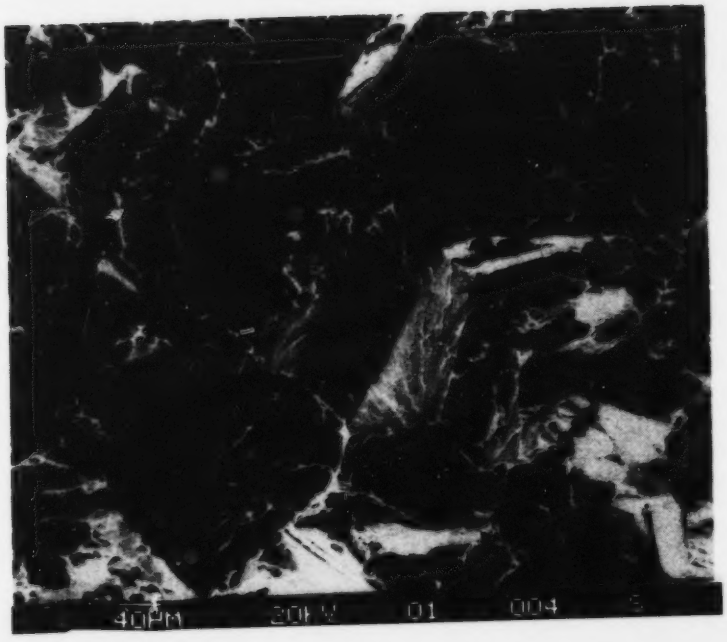

(b) 4 kJ/mm

Fig. 7. SEM fractographs showing cleavage facets for simulated CGHAZ of HSLA80 steel.

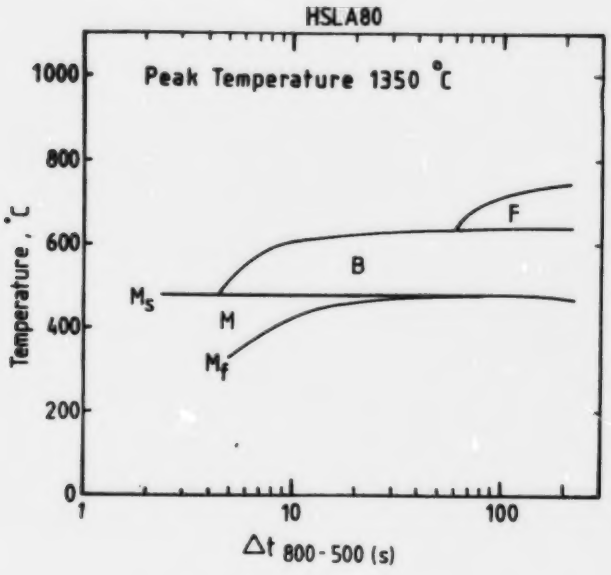

Fig. 8. CCT diagram of simulated CGHAZ of HSLA80 steel. (neg 15786)

(a) (neg 15914)

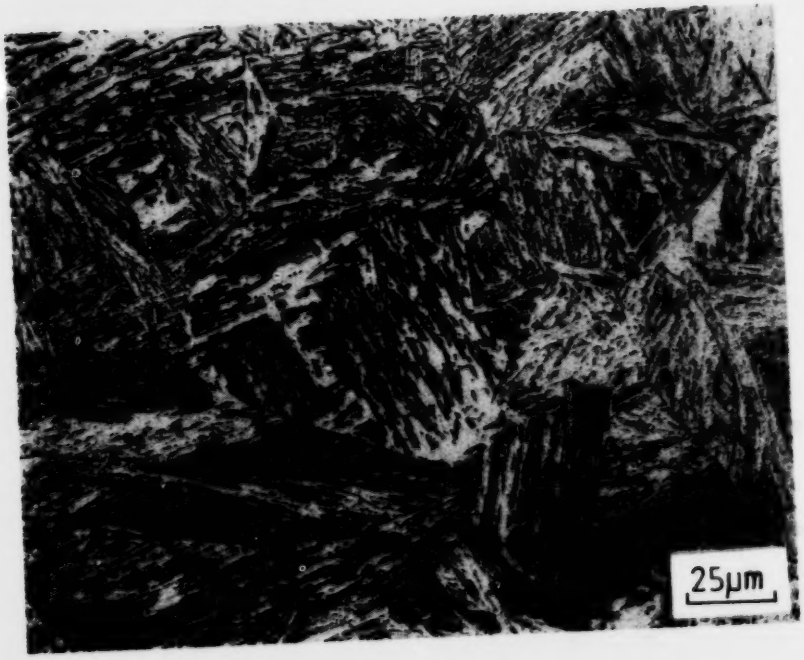

(b) (neg 15915)

Fig. 9. Optical micrographs of simulated CGHAZ of HSLA80. Δt 800-500 = 5s.

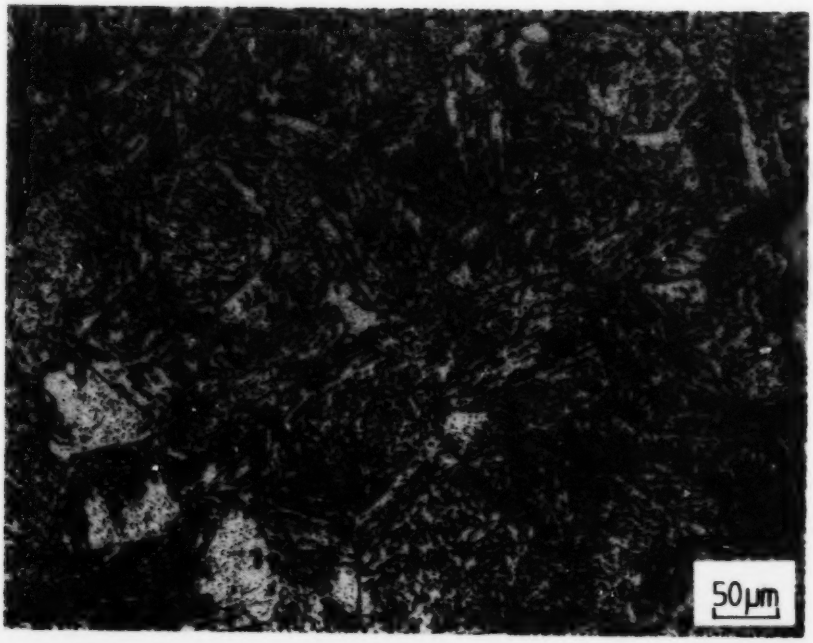

(a) (neg 15916)

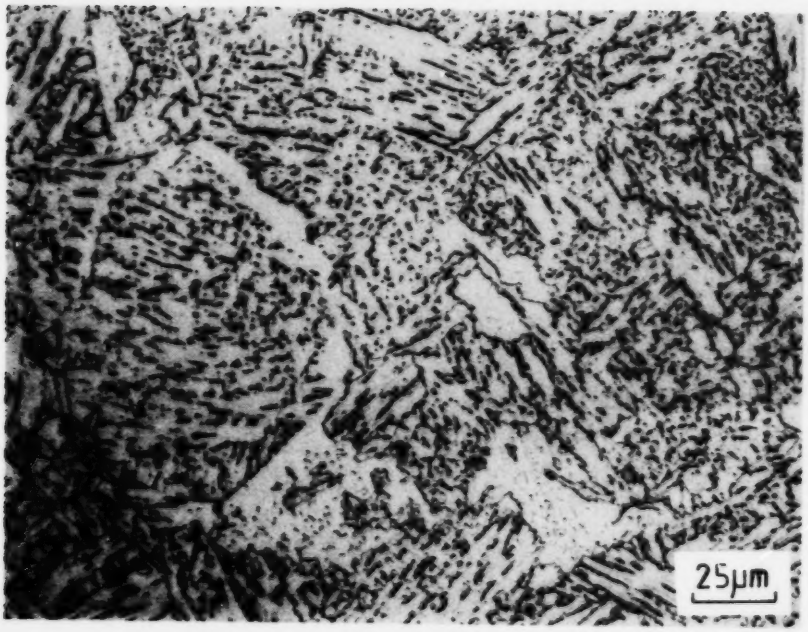

(b) neg 15917)

Fig. 10 Optical micrographs of simulated CGHAZ of HSLA80. $\Delta t_{800\text{-}500}$ =75s.